Nanoscale Horizons

Accepted Manuscript

This article can be cited before page numbers have been issued, to do this please use: Z. Nie, Y. Wang, Z. Li, Y. Sun, S. Qin, X. Liu, I. C. E. Turcu, Y. Shi, R. Zhang, Y. Ye, Y. Xu, G. Cerullo and F. Wang, *Nanoscale Horiz.*, 2019, DOI: 10.1039/C9NH00045C.

ROYAL SOCIETY OF CHEMISTRY

rsc.li/nanoscale-horizons

View Article Online
DOI: 10.1039/C9NH00045C

Nanoscale Horizons

COMMUNICATION

Ultrafast free carrier dynamics in black phosphorus-molybdenum disulfide (BP/MoS_2) heterostructure

Received 00th January 20xx,
Accepted 00th January 20xx

DOI: 10.1039/x0xx00000x

www.rsc.org/

Zhonghui Nie,[a,b] Yuhan Wang,[a,b] Ziling Li,[c] Yue Sun,[a] Shuchao Qin,[a] Xiaoping Liu,[d] Edmond Turcu,[a] Yi Shi,[a] Rong Zhang,[a] Yu Ye,[c] Yongbing Xu,*[a] Giulio Cerullo*[e,f] and Fengqiu Wang*[a,b]

Investigating and manipulating photocarrier dynamics in van der Waals (vdW) heterostructures with type-II band alignment have being actively carried out because of their fundamental and technological significance. Despite remarkable progresses on the ultrafast dynamics of interlayer excitons in transition metal dichalcogenides (TMDs) heterostructures, transient behaviors of free photocarriers in vdW heterostructures, a critical process governing the performance of optoelectronic devices, remain poorly understood. In this work, ultrafast dynamics of photo-generated free carriers in a type-II black phosphorus-molybdenum disulfide (BP/MoS_2) heterostructure is studied. A remarkably reduced lifetime (~ 5 ps) of interlayer electron-hole (*e-h*) recombination has been found, compared with those of BP film (~ 130 ps) and other exciton-prevailed TMD heterostructures. More interestingly, this ultrafast interlayer recombination process can be well described by the Langevin model, and the large recombination rate is fundamentally linked to the high carrier mobility in BP. In addition, broadband measurements reveal that the interlayer recombination rate is insensitive to the broad energy distribution of photocarriers. Our findings provide important and complementary new insights into the fundamental photo-physics of vdW heterostructures, and represent a novel proposal for designing broadband high-speed optoelectronic devices.

Concept Insights

Van der Waals (vdW) heterostructures with type-II band alignment hold great promise for applications in the fields of optoelectronics, photonics and spin-valleytronics. Photocarrier dynamics in such systems has been actively studied for guidance on improving device performance. However, current research efforts mostly focus on (interlayer) excitons, while it is the free carriers that ultimately determine the photocurrent and critically affect the performance of photo-sensitive devices. In addition, the rarely studied free carrier dynamics may offer complementary insights that may help elucidate the rather complicated exciton dynamics. Herein, we investigate the ultrafast dynamics of photo-generated free carriers in a type-II vdW heterostructure, constructed by black phosphorus (BP) and molybdenum disulfide (MoS_2). An unusually fast interlayer recombination (~ 5ps) of unbound photocarriers has been identified, which can be well described by a simple Langevin model. The large recombination rate is found to be fundamentally linked to the high carrier mobility in BP, suggesting effective pathways for carrier lifetime tuning. The present study not only reveals generic free carrier dynamics in 2D semiconductor heterostructures, but also provides new perspectives for interpreting the exciton dynamics in vdW heterostructures, both of which are crucial for designing high-speed novel devices based on 2D materials.

Introduction

Van der Waals (vdW) heterostructures with a type-II band alignment,[1,2] formed by stacks of two-dimensional (2D) materials, have attracted great attention in recent years as an excellent platform to explore exotic physics[3-9] and novel atomically-thin devices.[10-14] A comprehensive understanding on the dynamical evolution of photocarriers in vdW heterostructures is the prerequisite to control and optimize the performance of related optoelectronic devices, on which rapid advancements have been achieved.[15-23] On short timescales (< 1 ps), the photo-generated charge carriers transfer across the interface due to the built-in field within several tens of femtoseconds regardless of the relative crystallographic alignment;[16,20-23] on longer timescales (> 1 ps), the separated photocarriers recombine on a timescale varying from picoseconds to nanoseconds.[18,19,22] However, so far most experimental investigations focus on the charge transfer and recombination dynamics of interlayer excitons in transition

[a] School of Electronic Science and Engineering, Nanjing University, Nanjing 210023, China. Email: fwang@nju.edu.cn; ybxu@nju.edu.cn
[b] Key Laboratory of Intelligent Optical Sensing and Manipulation, Ministry of Education, Nanjing University, Nanjing 210093, China
[c] Department of Physics, Peking University, Beijing 100871, China
[d] College of Engineering and Applied Sciences, Nanjing University, Nanjing 210093, China
[e] Dipartimento di Fisica, Politecnico di Milano, Piazza Leonardo da Vinci 32, I-20133 Milano, Italy
[f] Istituto di Fotonica e Nanotecnologie (IFN), CNR, Piazza Leonardo da Vinci 32, I-20133 Milano, Italy. Email: giulio.cerullo@fisi.polimi.it

Electronic Supplementary Information (ESI) available: [details of any supplementary information available should be included here]. See DOI: 10.1039/x0xx00000x

View Article Online
DOI: 10.1039/C9NH00045E

metal dichalcogenides (TMDs) heterostructures,[16,18-23] while in fact the photocurrent in most optoelectronic devices arises from free carriers and interlayer exciton cannot form photocurrent until dissociating into free carriers.[10-14,24,25] In addition, most existing theoretical models[10,23] on the recombination dynamics do not fully account for the excitonic effect in low-dimensional materials[4,9,] and a number of experimental observations in the exciton-prevailed heterostructures remain to be elucidated.[20,22,29] Meanwhile, a heterostructure supporting free carriers may be more rigorously depicted by present theoretical mechanisms and the obtained complementary insights can be valuable in explaining the relatively complicated dynamics in exciton-dominated systems. To the best of our knowledge, so far there has been few investigations on the dynamic behaviours of free carriers in 2D semiconductor heterostructures.

Here, we chose to experimentally investigate the photocarrier dynamics of a vdW heterostructure supporting free carriers: a black phosphorus-molybdenum disulfide (BP/MoS_2) heterostructures with a type-II band alignment, as shown in the top panel of Fig. 1(a).[30,31] Compared with TMDs, the binding energy between charge carriers in BP film is much weaker (<40 meV) and unbound (quasi-)free carriers can be directly injected by optical excitation,[32,33] as shown in Fig. 1(a). In addition, BP-based vdW heterostructures are capable of extending the spectra range of 2D optoelectronic devices into the infrared (IR) range.[32,34-38] The direct and tunable bandgap spanning from visible to mid-IR, together with its much higher carrier mobility compared with TMDs and the anisotropy of physical properties, makes BP a highly versatile candidate for 2D optoelectronic and photonic devices especially for the IR range.[34-40]

In this study, femtosecond transient absorption spectroscopy is employed to investigate the dynamics of photo-generated free carriers in the BP/MoS_2 heterostructure. In addition to observing ultrafast electron transfer to MoS_2 after photoexciting the BP film, an unusually short lifetime of ~ 5 ps of the transferred electrons has been identified, much shorter than those of the constituent materials and the exciton-dominated heterostructures. Combining with the probing of the lifetime of holes remaining in the BP film, we find that this fast decay of interlayer free carriers can be well described by the Langevin model. The significant reduction of lifetime (from hundreds of picoseconds to several picoseconds) can be understood by considering a dramatically enhanced Langevin constant, caused by the high hole mobility of BP. Furthermore, broadband pump-probe spectroscopy demonstrates interlayer recombination rate of the free photocarriers is insensitive to their energy distribution. Our results suggest that in contrast to that of the exciton-dominated systems, the free carrier dynamics in 2D semiconductor heterostructures can be reasonably well depicted by a simple Langevin model. A new strategy is found to drastically reduce the photocarrier lifetime through engineering the Langevin constant at the heterointerface, which may have practical implications for designing broadband high-speed optoelectronic and photovoltaic devices based on 2D heterostructures.

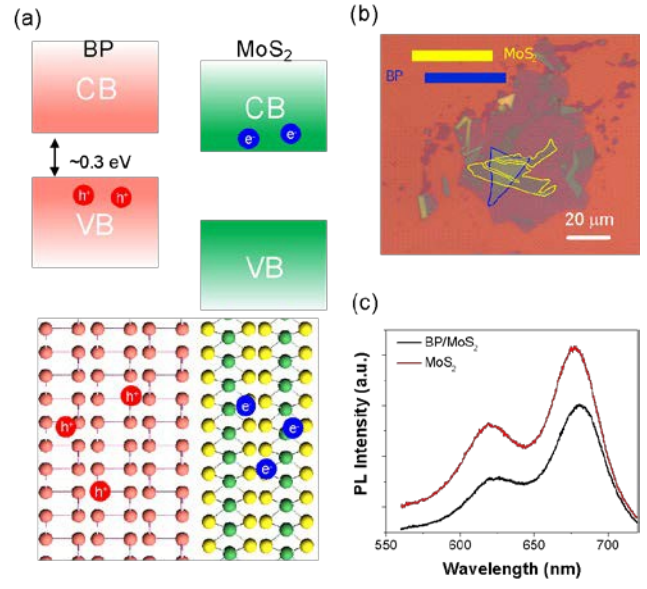

Fig. 1 (a) Illustration of the band alignment of the BP/MoS_2 heterostructure, which belongs to the Type-II heterostructure. Such a band structure can easily separate electrons and holes into different layers. (b) Optical microscope image of the BP/MoS_2 heterostructure, where the blue and yellow lines outline the BP film and the bilayer MoS_2 respectively. The scale bar is 20 μm. It should be noted that a thin hBN film (not marked) was used to protect the BP film from degradation. (c) Photoluminescence spectra of MoS_2 and the heterostructure under 514 nm laser excitation. PL quenching has been observed, which is attributed to interlayer charge transfer in the heterostructure.

Experimental

The BP and the MoS_2 films were mechanically exfoliated and stacked onto a silicon substrate with a 280-nm oxide layer to form a heterostructure as shown in Fig. 1(b). To avoid degradation of the BP film, a thin boron nitride (BN) film was used to cover the whole heterostructure. The thicknesses of the BP and MoS_2 films are ~8 and 1.1 nm, respectively, as measured by atomic force microscopy (AFM) shown in Fig. S1. The layer number of the BP film is estimated to be ~15, corresponding to a bandgap of 0.3 eV and a binding energy below 40 meV.[33,35,41] The layer thickness measured for the MoS_2 film is close to that of the bilayer sample (1.3 nm) and the difference between E^1_{2g} and A_{1g} Raman modes (shown in Fig. S2) is about 23 cm^{-1}, indicating that the sample is bilayer MoS_2.[4,42] Raman spectra of the BP film, bilayer MoS_2 and the heterostructure are presented in Fig. S3. These Raman modes associated with the individual materials have also been observed in the region of the heterostructure, which is consistent with previous reports[31,36] and suggests a good sample quality. In addition, because the A^2_g mode of BP film originates from the in-plane atomic motion, its Raman intensity exhibits polarization dependence.[43] The crystal orientation of BP film can be easily identified through polarization-dependent Raman spectroscopy, as reported in Fig. S4. Photoluminescence (PL) spectra of the bilayer MoS_2 and the heterostructure are presented in Fig. 1(c). The peaks at 680 nm and 620 nm of the MoS_2 (red line) arise from the A and B excitons.[4,42] Noticeable reduction (~30%) of PL intensity has

been observed in the heterostructure region, which is a typical signature for charge transfer in type-II heterostructures.[30,31] The ~30% decrease is not significant compared with that of other TMD-based heterostructures, and the main reasons could be the low PL efficiency of bilayer MoS_2 and the blocking of photo-excited hole transfer from MoS_2 to BP film by the majority carriers in BP film (holes) with high density.[36,39]

The ultrafast photocarrier response of the BP/MoS_2 heterostructure was directly monitored by transient differential reflection spectroscopy (details in Fig. S5 and Supplementary Note 1). An 800 nm (1.55 eV) linearly polarized laser, with 100 fs pulse duration, worked as the pump beam to excite photocarriers in the heterostructure. Due to the energy band alignment as well as the layer thickness, pump pulses should be primarily absorbed by the BP film, as confirmed by our experiments on the MoS_2 bilayer.[4,42,44] Using a 0.4%/nm absorption rate at 800 nm for BP film[41] and assuming each absorbed photon excites one *e-h* pair, the peak density of photocarriers excited in the BP can reach a value of ~10^{12} cm^{-2} and these photocarriers should be free carriers rather than excitons considering the low binding energy inside BP. To observe the electron transfer from the conduction band (CB) of BP film to the CB of MoS_2, we adopted a 620 nm laser to probe the dynamical behaviours of electrons in MoS_2, as illustrated in Fig. 2(a). As the photon energy of the pump pulse (1.55 eV) is smaller than that of the probe pulse (2 eV) and the absorption gap of MoS_2 (1.88 eV), individual BP and MoS_2 films yielded no detectable signals, as shown in Fig. 2(b). However, an ultrafast and intense photo-bleaching (PB) signal has been observed in the heterostructure region, depicted by the black dots in Fig. 2(b). While the ultrafast interlayer electron transfer is not directly resolvable due to the limited instrumental response (~ 300-400 fs),[16,20,22,45] a remarkable observation is the extremely short carrier relaxation time of ~5±0.2 ps. (Single-exponential fitting is shown by the red line in Fig. 2(b).) Such a short lifetime is not only at least one order of magnitude faster than the intrinsic lifetimes of photocarriers in individual MoS_2 and BP film (as shown in Fig. S6),[18,22,41,46-48] but also strikingly distinct from those of the long-lived interlayer excitons in the TMD heterostructures.[18,22] To explore the origin of such fast relaxation process, power-dependent measurements have been carried out. We extracted the peak values of the ΔR/R signal from the dynamic curves and summarized them as a function of pump fluence, as illustrated in the top panel of Fig. 2(c). Clearly, below the pump fluence of ~80 μJ/cm^2 (photocarrier density of ~10^{13} cm^{-2}), the transient signal increases linearly with the incident power density, while for higher fluences it displays a saturation behavior.[38,43,44] Interestingly, the lifetime of the transferred electrons in MoS_2 stays almost constant (~5 ps) (shown in the bottom panel of Fig. 2(c)), and exhibits negligible dependence on injected photocarrier density even beyond the linear region, indicating that such short electron lifetime should not arise from trapping by interfacial defects.[49]

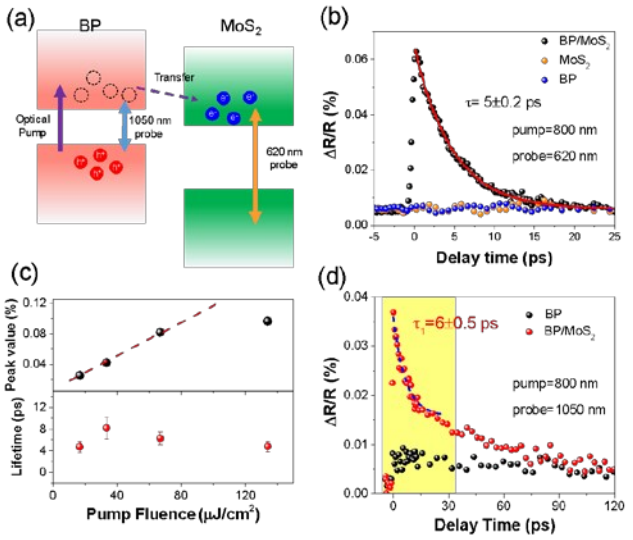

Fig. 2 (a) Schematic diagram illustrating the transient processes occurring in a BP/MoS_2 heterostructure when the probe wavelengths are 620 nm and 1050 nm, respectively. (b) Transient reflectivity signals of the BP/MoS_2 heterostructure and its constituent layers when pumped at 800 nm and probed at 620 nm. The ultrafast signal build-up of the heterostructure proves the existence of electron transfer, and the ~ 5 ps relaxation time is much shorter than those of photocarriers in individual MoS_2 and BP. (c) Pump-fluence dependence of the maximum ΔR/R signal (top) and lifetime (bottom) when the pump and probe wavelengths are 800 nm and 620 nm respectively. (d) Time-resolved differential reflection measured for the BP film and BP/MoS_2 heterostructure with an 800 nm pump and a 1050 nm probe.

To reveal more details of the relaxation mechanisms, we changed the probe wavelength to 1050 nm (~ 1.2 eV) while fixing the pump wavelength at 800 nm. As its photon energy is far below the bandgap of MoS_2, the probe pulse then primarily detected transient signal from holes in the BP film, as is illustrated by Fig. 2(a). The measured transient signals of the BP film and the heterostructure are presented in Fig. 2(d). The transient signal of the BP film can be well fitted by a time constant of 130 ps (see Fig. S6), in agreement with the previously reported lifetime of free carriers in BP.[41,47,48] Meanwhile, much stronger PB signal has been observed for the heterostructure, show in Fig. 2(d), whose magnitude is comparable to the signal induced by transferred electrons in MoS_2 (Fig. 2(b)), and 3-4 times larger than that of the individual BP. Such large enhancement in signal is tentatively ascribed to the increase of screening effect and similar phenomenon has also been found in a graphene/WS_2 heterostructure.[17] Noticeably, a fast relaxation component (yellow shaded area) clearly emerges in the dynamic curve of the heterostructure with a time constant of ~6±0.5 ps, well corresponding to the lifetime of holes' population in the BP film. It should be noted that the observed ultrashort lifetime of holes in BP film coincides with that of the transferred electrons in MoS_2, which strongly suggests that there exists an efficient bimolecular recombination process between photocarriers across the interface.

In the vdW heterostructures, there are two mechanisms potentially contributing to this unusual interlayer *e-h* recombination: Shockley-Read-Hall (SRH) recombination (assisted by traps or defect states) and Langevin recombination

View Article Online
DOI: 10.1039/C9NH00456C

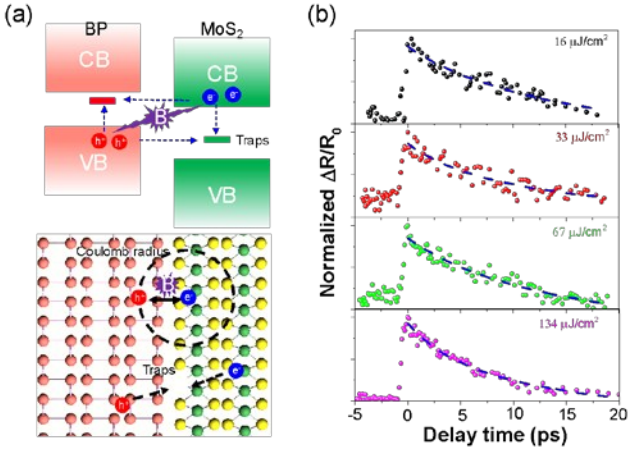

Fig. 3 (a) Two potential interlayer recombination mechanisms. In the top panel, the blue and purple arrows indicate SRH and Langevin recombination processes, respectively. The circle in the bottom panel conceptually marks the Coulomb radius, according to the Langevin model, of an electron at the heterointerface. The dashed arrows point to an interfacial defect which may act as a SRH recombination centre for charge carriers. (b) Transient signals when pump=800 nm and probe=620 nm measured at different pump fluences. The dashed blue lines are the fitting results using the rate equation based on Langevin model (Equation S(1)).

(mediated by interlayer Coulomb interaction), as illustrated in Fig. 3(a).[10,50,51] The coexistence of these two mechanisms has been previously reported in TMD heterostructures devices, and both of them made significant contributions to the interlayer recombination, significantly affecting the formation of photocurrent and the efficiency of photon-electron conversion.[10-14] In our case, the trap-assisted SRH recombination can be ruled out as the dominant process by the observed pump fluence-independence of photocarrier lifetimes. In contrast, the Langevin model describing the simultaneous recombination between electrons and holes is more consistent with our observations in Fig. 2. The Langevin model could be applicable here with another important reason being the enhanced Coulomb interaction between photocarriers confined in low-dimensional systems.

The rate equation based on Langevin recombination can be expressed as:[10,50]

$$\frac{d\Delta n}{dt} = G - B \times (n_0 + \Delta n) \times (p_0 + \Delta p)^s$$

where G is the rate of photocarriers generation, B is the Langevin recombination constant, n_0 and p_0 are the intrinsic densities of electrons in MoS_2 and holes in BP, and Δn and Δp are photo-generated electron and hole densities. An exponent s ($1.2<s<1.5$) is typically used to account for the 2D case.[51] It should be noted that besides the photo-generated carrier density, the intrinsic carrier densities in BP and MoS_2, whose influence on photocarrier recombination is usually neglected in previous analysis, also play a role in the rate equation above. The temporal evolution of photocarrier density is given by Equation S(1) in SI, a simplified solution of the above rate equation. As shown by Fig. 3(b), the transient reflectivity signals at different pump fluences can be well reproduced by Equation S(1) when a typical value of 1.2 is adopted for s,[10,50,51] indicating the dominance of Langevin process in this system. The fitted values of the intrinsic carrier densities for BP and MoS_2 ~ (4.9±0.5) $\times 10^{12}$ cm^{-2} are close to previously reported values.[10,36,52] The dominance of Langevin model distinguishes the recombination dynamics in the studied BP/MoS_2 system from those in TMD heterostructures, and this difference could result from the binding degree (free carriers or excitons) of interlayer photocarriers in vdW heterostructures. Moreover, the Langevin recombination constant B is extracted to be ~(2.33±0.25)$\times 10^{-10}$ m^2/s, much larger than the reported value of a MoS_2/WSe_2 heterostructure (B ~ 4.0×10^{-13} m^2/s when s=1.2).[10] As demonstrated by the expression of B (Equation S(2) in SI), this constant is proportional to the carrier mobilities in constituent layers. Considering the much higher mobility of holes in BP compared with TMDs, the large discrepancy between B in these two systems could be mainly accounted for by the difference in carrier mobility. In addition, since the rate of Langevin recombination essentially depends on the probability of electrons and holes meeting each other in coordinate space, the unbound nature of interlayer free carriers in BP/MoS_2 heterostructure could also partially contribute to the much larger Langevin constant.

Therefore, we attribute the observed ultrashort lifetime of photocarriers at the BP/MoS_2 interface to an efficient Langevin recombination process, with contributions from high (intrinsic) carrier densities in the two constituent materials and a large recombination constant B. Our findings indicate that the carrier density and mobility, as well as the binding degree of photocarriers together determine the photocarrier dynamics in BP/MoS_2 heterostructure and could provide effective approaches for tailoring the photocarrier lifetime in a type-II 2D

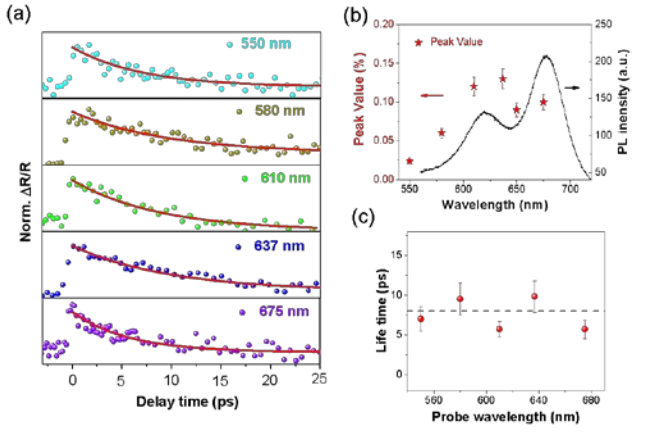

Fig. 4 Broadband ultrafast nonlinear optical properties of BP/MoS_2 heterostructure. (a) The ultrafast pump-probe measurements with a probe wavelength varying from 550 nm to 675 nm, covering the A and B exciton peaks, when pump wavelength is fixed at 800 nm. Coloured dots are experimental data and red solid lines correspond to single-exponential fitting results. (b) Peak values of ΔR/R signal in the heterostructure under different probe wavelengths (red stars, left axis), extracted from (a). For comparison, the PL spectrum (black line, right axis) of the bilayer MoS_2 is also drawn, suggesting that exciton states in MoS_2 may affect the distribution of the transferred electrons. (c) The lifetime extracted from signals in (a) by single-exponential fitting as a function of probe wavelength. The lifetime of the heterostructure remains insensitive to the change of probe wavelength.

heterostructure and the photo-response of related optoelectronic devices, *e.g.*, gate-control,[53] chemical doping[54] or substrate-induced screening.[53] Further experimental and theoretical studies may be useful to clarify the effects from other potential contributing mechanisms, such as interlayer coupling or electronic-state hybridization.[55]

To further investigate the energy distribution of transferred electrons and its influence on the Langevin recombination dynamics, broadband ultrafast spectroscopy has been performed. The probe wavelength was tuned from 550 nm (2.25 eV) to 675 nm (1.84 eV), covering the A and B excitonic peaks of MoS_2, while the pump wavelength was fixed at 800 nm. The measured differential reflectivity dynamics of BP/MoS_2 heterostructure are shown in Fig. 4(a), with the red lines indicating the single-exponential fittings. Firstly, the observation of transient signals for all probe wavelengths suggest that the transferred electrons occupy a broad spread of energy states in the CB of MoS_2. This phenomenon agrees with some recent theoretical and experimental results, where hot electrons are able to transfer from conduction band minimum (CBM) of one layer to energy levels above the CBM of the other layer.[26,56] Interestingly, broadband PB signals are observed for the first time, in contrast to the alternation between photo-absorption (PA) and PB as a result of broadening and redshift of exciton absorption in TMD heterostructures. Secondly, the excess energy available to the transferred electrons could induce a thermalization process. The peak values of the transient signals in Fig. 4(a) are extracted and plotted as a function of the probe wavelengths in Fig. 4(b). The trend of peak values roughly follows that of the PL spectrum of MoS_2 (the black solid line), confirming that thermal distribution of electrons is established on an ultrafast timescale.[56,57] These observations mean that the ultrashort rising time (300-400 fs) in Fig. 4(a) covers both the electron transfer and thermalization processes. Then we examined the relationship between electron lifetime and the probe wavelength, as shown in Fig. 4(c). Interestingly, the lifetime varying between 5 and 8 ps shows no obvious dependence on the probe wavelength, which suggests that the rate of interlayer Langevin recombination is not sensitive to kinetic energy of electrons. Besides the energy distribution, we also investigated the polarization dependence of the transferred electrons and found that the anisotropy of photocarriers in the heterostructure has been partially weakened, compared with that of individual BP film (Supplementary Note 3).

Combining all our measurements, the transient photocarrier process in the BP/MoS_2 heterostructure can be characterized by three major steps: the generation of hot e-h pairs in BP through optical excitation; ultrafast interlayer charge separation (electrons transfer to the MoS_2 layers while holes are left in the BP layers) and thermalization (redistribution among the CB of MoS_2) within few hundreds of femtoseconds, and finally the Langevin recombination between the separated electrons and holes in different layers on a timescale of ~5 ps. The response time of BP-based photodetectors is generally limited by the intrinsic lifetime of photocarriers (up to hundreds of picoseconds) and such a significant reduction of photocarrier lifetime in the BP/MoS_2 heterostructure, close to that of graphene,[58] makes it possible to construct BP based heterostructures to realize novel IR photo-sensitive devices with high speed.

Conclusions

In conclusion, we have investigated the ultrafast dynamics of photoexcited free carriers in a BP/MoS_2 heterostructure by two-color ultrafast pump-probe optical spectroscopy. In addition to observing ultrafast charge transfer, we found an unusually short lifetime of ~5 ps of the interlayer photocarriers, significantly shorter than those of pure BP film and TMD heterostructures. Supported by experimental and theoretical analysis, we attributed the observed ultrafast relaxation of interlayer free carriers to the Langevin recombination with a significantly enhanced Langevin constant *B*, due to the much higher hole mobility in BP. Moreover, broadband measurements revealed a relatively broad energy distribution of transferred electrons in MoS_2. The broadband PB signals with similar lifetimes demonstrated the energy-independent recombination processes of interlayer free carries. Our findings provide new insights into the fundamental photo-physics in vdW heterostructures and point out a new route to dramatically shorten photocarrier lifetimes at 2D heterointerface, promoting the development of ultrafast optoelectronic devices in the IR range.

Conflicts of interest

There are no conflicts to declare.

Authors' contributions

F.W., G.C. and Y.X. conceived the project and provided the experimental analysis. Z.N. and Y.W. performed the ultrafast measurements and basic characterizations of the samples; Z.L. and Y.Y. prepared the samples; Y.S., S.Q., X.L., E.T., Y.S. and R.Z. provided help and useful advice during ultrafast measurements. The manuscript was written through contributions of all authors. All authors have given approval to the final version of the manuscript.

Acknowledgements

This work was supported by The State Key Project of Research and Development of China (2017YFA0206304); National Basic Research Program of China (2014CB921101, 2011CB301900); National Natural Science Foundation of China (61775093, 61427812); National Young 1000 Talent Plan; A 'Jiangsu Shuangchuang Team' Program; Natural Science Foundation of Jiangsu Province (BK20170012). And G.C. also acknowledged support by the European Union's Horizon 2020 research and innovation program under grant agreement No 785219 (GrapheneCore2).

References

1 A. K. Geim and I. V. Grigorieva, *Nature*, 2013, **499**, 419-425.
2 K. S. Novoselov, A. Mishchenko, A. Carvalho and A. H. Castro Neto, *Science*, 2016, **353**, aac9439.
3 L. Britnell, R. M. Ribeiro, A. Eckmann, R. Jalil, B. D. Belle, A. Mishchenko, Y. J. Kim, R. V. Gorbachev, T. Georgiou, S. V. Morozov, A. N. Grigorenko, A. K. Geim, C. Casiraghi, A. H. Castro Neto and K. S. Novoselov, *Science*, 2013, **340**, 1311-1314.
4 K. F. Mak, C. Lee, J. Hone, J. Shan and T. F. Heinz, *Phys. Rev. Lett.* 2010, **105**, 136805.
5 C. R. Dean, L. Wang, P. Maher, C. Forsythe, F. Ghahari, Y. Gao, J. Katoch, M. Ishigami, P. Moon, M. Koshino, T. Taniguchi, K. Watanabe, K. L. Shepard, J. Hone and P. Kim, *Nature*, 2013, **497**, 598-602.
6 E. Wang, X. Lu, S. Ding, W. Yao, M. Yan, G. Wan, K. Deng, S. Wang, G. Chen, L. Ma, J. Jung, A. V. Fedorov, Y. Zhang, G. Zhang and S. Zhou, *Nat. Phys.* 2016, **12**, 1111-1115.
7 C. Jin, J. Kim, J. Suh, Z. Shi, B. Chen, X. Fan, M. Kam, K. Watanabe, T. Taniguchi, S. Tongay, A. Zettl, J. Wu and F. Wang, *Nat. Phys.* 2016, **13**, 127-131.
8 J. Zhang, J. Wang, P. Chen, Y. Sun, S. Wu, Z. Jia, X. Lu, H. Yu, W. Chen, J. Zhu, G. Xie, R. Yang, D. Shi, X. Xu, J. Xiang, K. Liu and G. Zhang, *Adv. Mater.* 2016, **28**, 1950-1956.
9 A. Raja, A. Chaves, J. Yu, G. Arefe, H. M. Hill, A. F. Rigosi, T. C. Berkelbach, P. Nagler, C. Schuller, T. Korn, C. Nuckolls, J. Hone, L. E. Brus, T. F. Heinz, D. R. Reichman and A. Chernikov, *Nat. Commun.* 2017, **8**, 15251.
10 C. H. Lee, G. H. Lee, A. M. van der Zande, W. Chen, Y. Li, M. Han, X. Cui, G. Arefe, C. Nuckolls, T. F. Heinz, J. Guo, J. Hone and P. Kim, *Nat. Nanotechnol.* 2014, **9**, 676-681.
11 F. Barati, M. Grossnickle, S. Su, R. K. Lake, V. Aji and N. M. Gabor, *Nat. Nanotechnol.* 2017, **12**, 1134-1139.
12 M. M. Furchi, A. Pospischil, F. Libisch, J. Burgdorfer and T. Mueller, *Nano Lett.* 2014, **14**, 4785-4791.
13 M. Long, E. Liu, P. Wang, A. Gao, H. Xia, W. Luo, B. Wang, J. Zeng, Y. Fu and K. Xu, *Nano Lett.* 2016, **16**, 2254-2259.
14 H. Xue, Y. Wang, Y. Dai, W. Kim, H. Jussila, M. Qi, J. Susoma, Z. Ren, Q. Dai, J. Zhao, K. Halonen, H. Lipsanen, X. Wang, X. Gan and Z. Sun, *Adv. Funct. Mater.* 2018, **28**, 1804388.
15 C. Jin, E. Y. Ma, O. Karni, E. C. Regan, F. Wang and T. F. Heinz, *Nat. Nanotechnol.* 2018, **13**, 994-1003.
16 X. Hong, J. Kim, S. F. Shi, Y. Zhang, C. Jin, Y. Sun, S. Tongay, J. Wu, Y. Zhang and F. Wang, *Nat. Nanotechnol.* 2014, **9**, 682-686.
17 J. He, N. Kumar, M. Z. Bellus, H. Y. Chiu, D. He, Y. Wang and H. Zhao, *Nat. Commun.* 2014, **5**, 5622.
18 P. Rivera, J. R. Schaibley, A. M. Jones, J. S. Ross, S. Wu, G. Aivazian, P. Klement, K. Seyler, G. Clark, N. J. Ghimire, J. Yan, D. G. Mandrus, W. Yao and X. Xu, *Nat. Commun.* 2015, **6**, 6242.
19 F. Ceballos, M. Z. Bellus, H. Y. Chiu and H. Zhao, *ACS Nano*, 2014, **8**, 12717-12724.
20 Z. Ji, H. Hong, J. Zhang, Q. Zhang, W. Huang, T. Cao, R. Qiao, C. Liu, J. Liang, C. Jin, L. Jiao, K. Shi, S. Meng and K. Liu, *ACS Nano*, 2017, **11**, 12020-12026.
21 F. Ceballos, M. G. Ju, S. D. Lane, X. C. Zeng and H. Zhao, *Nano Lett.* 2017, **17**, 1623-1628.
22 H. Zhu, J. Wang, Z. Gong, Y. D. Kim, J. Hone and X. Y. Zhu, *Nano Lett.* 2017, **17**, 3591-3598.
23 Q. Zheng, W. A. Saidi, Y. Xie, Z. Lan, O. V. Prezhdo, H. Petek and J. Zhao, *Nano Lett.* 2017, **17**, 6435-6442.
24 G. Lee, S. J. Pearton, F. Ren and J. Kim, *ACS Appl. Mater. Interfaces* 2018, **10**, 10347-10352.
25 T. Hong, B. Chamlagain, T. Wang, H. J. Chuang, Z. Zhou and Y. Q. Xu, *Nanoscale*, 2015, **7**, 18537-18541.
26 P. Kambhampati, *Acc. Chem. Res.* 2011, 44, 1-13.
27 P. Kambhampati, *J. Phys. Chem. C.* 2011, 115, 22089-22109.
28 P. Kambhampati, *J. Phys. Chem. Lett.* 2012, 3, 1182-1190.
29 X. Zhu, N. R. Monahan, Z. Gong, H. Zhu, K. W. Williams and C. A. Nelson, *J. Am. Chem. Soc.* 2015, **137**, 8313-8320.
30 Y. Deng, Z. Luo, N. J. Conrad, H. Liu, Y. Gong, S. Najmaei, P. M. Ajayan, J. Lou, X. Xu and P. D. Ye, *ACS Nano*, 2014, **8**, 8292-8299.
31 J. Yuan, S. Najmaei, Z. Zhang, J. Zhang, S. Lei, M. A. P, B. I. Yakobson and J. Lou, *ACS Nano*, 2015, **9**, 555-563.
32 L. Li, J. Kim, C. Jin, G. J. Ye, D. Y. Qiu, F. H. da Jornada, Z. Shi, L. Chen, Z. Zhang, F. Yang, K. Watanabe, T. Taniguchi, W. Ren, S. G. Louie, X. H. Chen, Y. Zhang and F. Wang, *Nat. Nanotechnol.* 2017, **12**, 21-25.
33 G. Zhang, A. Chaves, S. Huang, F. Wang, Q. Xing, T. Low and H. Yan, *Sci. Adv*. 2018, **4**, eaap9977.
34 H. Yuan, X. Liu, F. Afshinmanesh, W. Li, G. Xu, J. Sun, B. Lian, A. G. Curto, G. Ye, Y. Hikita, Z. Shen, S. C. Zhang, X. Chen, M. Brongersma, H. Y. Hwang and Y. Cui, *Nat. Nanotechnol.* 2015, **10**, 707-713.
35 X. Wang, A. M. Jones, K. L. Seyler, V. Tran, Y. Jia, H. Zhao, H. Wang, L. Yang, X. Xu and F. Xia, *Nat. Nanotechnol.* 2015, **10**, 517-521.
36 F. Xia, H. Wang and Y. Jia, *Nat. Commun.* 2014, **5**, 4458.
37 M. Huang, M. Wang, C. Chen, Z. Ma, X. Li, J. Han and Y. Wu, *Adv. Mater.* 2016, **28**, 3481-3485.
38 L. Viti, J. Hu, D. Coquillat, A. Politano, C. Consejo, W. Knap and M. S. Vitiello, *Adv. Mater.* 2016, **28**, 7390-7396.
39 L. Li, Y. Yu, G. J. Ye, Q. Ge, X. Ou, H. Wu, D. Feng, X. H. Chen and Y. Zhang, *Nat. Nanotechnol.* 2014, **9**, 372-377.
40 Y. Liu, T. Low and P. P. Ruden, *Phys. Rev. B* 2016, **93**.
41 S. Ge, C. Li, Z. Zhang, C. Zhang, Y. Zhang, J. Qiu, Q. Wang, J. Liu, S. Jia, J. Feng and D. Sun, *Nano Lett.* 2015, **15**, 4650-4656.
42 P. Tonndorf, R. Schmidt, P. Bottger, X. Zhang, J. Borner, A. Liebig, M. Albrecht, C. Kloc, O. Gordan, D. R. T. Zahn, S. M. de Vasconcellos and R. Bratschitsch, *Opt. Express* 2013, **21**, 4908-4916.
43 X. Ling, S. Huang, E. H. Hasdeo, L. Liang, W. M. Parkin, Y. Tatsumi, A. R. Nugraha, A. A. Puretzky, P. M. Das, B. G. Sumpter, D. B. Geohegan, J. Kong, R. Saito, M. Drndic, V. Meunier and M. S. Dresselhaus, *Nano Lett.* 2016, **16**, 2260-2267.
44 T. Cheiwchanchamnangij and W. R. L. Lambrecht, *Phys. Rev. B* 2012, **85**.
45 M. Z. Bellus, Z. Yang, P. Zereshki, J. Hao, S. P. Lau and H. Zhao, *Nanoscale Horiz.* 2019, 4, 236-242.
46 V. Iyer, P. D. Ye and X. F. Xu, *2D Mater.* 2017, **4**.
47 R. J. Suess, M. M. Jadidi, T. E. Murphy and M. Mittendorff, *Appl. Phys. Lett.* 2015, **107**.
48 J. He, D. He, Y. Wang, Q. Cui, M. Z. Bellus, H. Y. Chiu and H. Zhao, *ACS Nano*, 2015, **9**, 6436-6442.
49 B. Liu, Y. Meng, X. Ruan, F. Wang, W. Liu, F. Song, X. Wang, J. Wu, L. He, R. Zhang and Y. Xu, *Nanoscale*, 2017, **9**, 18546-18551.
50 G. Juška, K. Genevičius, N. Nekrašas, G. Sliaužys and R. Österbacka, *Appl. Phys. Lett.* 2009, **95**, 013303.
51 N. C. Greenham and P. A. Bobbert, *Physical Review B*, 2003, **68**.
52 Z. Yu, Z. Y. Ong, Y. Pan, Y. Cui, R. Xin, Y. Shi, B. Wang, Y. Wu, T. Chen, Y. W. Zhang, G. Zhang and X. Wang, *Adv. Mater.* 2016, **28**, 547-552.
53 B. Radisavljevic, A. Radenovic, J. Brivio, V. Giacometti and A. Kis, *Nat. Nanotechnol.* 2011, **6**, 147-150.

View Article Online
DOI: 10.1039/C9NH00045C

54 M. Amani, D. H. Lien, D. Kiriya, J. Xiao, A. Azcatl, J. Noh, S. R. Madhvapathy, R. Addou, S. Kc, M. Dubey, K. Cho, R. M. Wallace, S. C. Lee, J. H. He, J. W. Ager, 3rd, X. Zhang, E. Yablonovitch and A. Javey, *Science*, 2015, **350**, 1065-1068.
55 N. R. Wilson, P. V. Nguyen, K. Seyler, P. Rivera, A. J. Marsden, Z. P. Laker, G. C. Constantinescu, V. Kandyba, A. Barinov, N. D. Hine, X. Xu and D. H. Cobden, *Sci. Adv*. 2017, **3**, e1601832.
56 H. Chen, X. Wen, J. Zhang, T. Wu, Y. Gong, X. Zhang, J. Yuan, C. Yi, J. Lou, P. M. Ajayan, W. Zhuang, G. Zhang and J. Zheng, *Nat. Commun.* 2016, **7**, 12512.
57 M. Massicotte, P. Schmidt, F. Vialla, K. Watanabe, T. Taniguchi, K. J. Tielrooij and F. H. Koppens, *Nat. Commun.* 2016, **7**, 12174.
58 P. A. George, J. Strait, J. Dawlaty, S. Shivaraman, M. Chandrashekhar, F. Rana and M. G. Spencer, *Nano Lett.* 2008, **8**, 4248-4251.

View Article Online
DOI: 10.1039/C9NH00045C

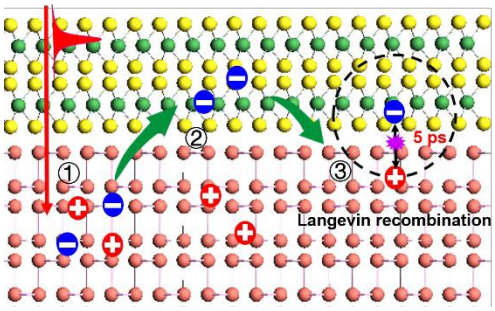

Free photocarriers in a BP/MoS_2 type-II vdW heterostructure are found to undergoes a usually fast Langevin interlayer recombination (~ 5 ps).